A New Approach for Benefit Evaluation of Multiterminal VSC–HVDC Using A Proposed Mixed AC/DC Optimal Power Flow

Wang Feng, *Student Member, IEEE*, Le Anh Tuan, *Member, IEEE*, Lina Bertling Tjernberg, *Senior Member, IEEE*, Anders Mannikoff, *Member, IEEE*, and Anders Bergman, *Senior Member, IEEE*

***Abstract*—In this paper, an extended optimal power-flow (OPF) model incorporating a detailed model of a voltage-source converter-based–multiterminal high-voltage direct current system (VSC–MTDC) is proposed, hereafter referred to as the mixed ac/dc OPF (M-OPF) model. A cost-benefit analysis approach using the M-OPF model as the calculation engine is proposed to determine the preferred VSC-MTDC alternative to be installed in an existing ac transmission system. In this approach, the operational benefits of VSC–MTDC systems are evaluated against their investment costs to derive the benefit-to-cost ratios (BCR) which reflect the cost-effectiveness of the alternatives. A case study has been carried out using a modified Nordic 32-bus system. The results of the study show that VSC–MTDC systems might lead to a reduction in total operation cost, and the reduction of the total system transmission loss depends to a large extent on the VSC–MTDC configuration. The results from sensitivity analyses show that if the VSC loss could be reduced to a third of the original level, the total benefit from the system would be increased by about 70%. A suggestion for the placement and configuration of a VSC–MTDC system is made based on calculated BCRs.**

***Index Terms*—AC/DC system, cost minimization, cost-benefit analysis, loss minimization, multiterminal VSC-HVDC, optimal power flow.**

NOMENCLATURE

Abbreviations:

HVDC	High voltage direct current.
LCC	Line-commutated converter.
MMC	Modular multilevel converter.
M − OPF	Mixed ac/dc OPF model.
OPF	Optimal power flow.
PCC	Point of common coupling.
PWM	Pulsewidth modulation.
VSC	Voltage-source converter.
VSC − HVDC	VSC-based HVDC.
VSC − MTDC	Multiterminal VSC-HVDC.

Constants:

A_{ci}	Cost coefficient of generator i[\$].
A_{li}	VSC loss coefficient of VSC i [in per unit (p.u.)].
B_r	Susceptance of VSC phase reactor (p.u.).
B_{ci}	Cost coefficient of generator i (MWh).
B_f	Susceptance of VSC filter (p.u.).
B_{ij}	Susceptance element of ac network admittance matrix (p.u.).
B_{li},	VSC loss coefficient of VSC i (p.u.).
C_{ci}	Cost coefficient of generator i [\$/MW^{2}h]
C_{li}	VSC loss coefficient of VSC i (p.u.).
$g_{i_{\rm dc}j_{\rm dc}}$	Conductance of dc cable $i_{\rm dc} - j_{\rm dc}$ (p.u.).
g_{ij}	Conductance of ac transmission line $i - j$ (p.u.).
$G_{i_{\rm dc}j_{\rm dc}}$	Conductance element of dc network admittance matrix (p.u.).
G_{ij}	Conductance element of ac network admittance matrix (p.u.).
k_Q	VSC reactive power lower limit factor.
k_v	Voltage relationship factor between VSC ac and dc buses.
Inv	Investment of VSC-MTDC system [M\$].
P_{di}	Active load at bus i (p.u.).
Q_{di}	Reactive load at bus i (p.u.).
r	Discount rate (in percentage).
R_r	Resistance of VSC phase reactor (p.u.).
R_{tr}	Resistance of VSC transformer (p.u.).

Manuscript received November 16, 2012; revised March 14, 2013; accepted May 21, 2013. Date of publication July 30, 2013; date of current version January 21, 2014. This work was supported in part by Chalmers Energy Initiative and in part by SP Technical Research Institute of Sweden. Paper no. TPWRD-01240-2012.

W. Feng, A. L. A. Tuan, and L. B. Tjernberg are with the Division of Electric Power Engineering, Chalmers University of Technology, Gothenburg 41296, Sweden (e-mail: feng.wang,tuan.le; lina.bertling@chalmers.se).

A. Mannikoff and A. Bergman are with SP Technical Research Institute of Sweden, Borås 501 15, Sweden (e-mail: anders.mannikoff@sp.se).

Color versions of one or more of the figures in this paper are available online at http://ieeexplore.ieee.org.

Digital Object Identifier 10.1109/TPWRD.2013.2267056

S_{base}	System base value of power [in megavolt-amperes (MVA)].
$S_{\rm nom}$	Nominal rating of VSC station (MVA).
t	Operation hours of each period.
V_{dcnom}	Nominal dc bus voltage (in kilovolts).
X_r	Reactance of VSC phase reactor (p.u.).
X_{tr}	Reactance of VSC transformer (p.u.) μ.

Variables:

BCR	Benefit-to-cost ratio.
$Cost$	Total generation cost ($M).
$C_1^{yr.p}$	Generation cost of the base case for period p and year yr ($M).
$C_2^{yr.p}$	Generation cost of the case with VSC-MTDC for period p and year yr ($M).
I_{vi}	Phase current of VSC valve of VSC i (p.u.).
$L_1^{yr.p}$	Power losses of the base case for period p and year yr (MW).
$L_2^{yr.p}$	Power losses of the case with VSC-MTDC for period p and year yr (MW).
P_{acloss}	Total active losses of ac transmission lines (p.u.).
P_c	Active power at VSC ac bus (p.u.).
$P_{\rm cdc}$	DC power at VSC dc bus (p.u.).
P_{dcloss}	Total active losses of dc cables (p.u.).
P_{gi}	Active power output from generator i (p.u.).
$P_{i_{\rm dc}}, P_{j_{\rm dc}}$	DC power at dc bus $i_{\rm dc}, j_{\rm dc}$ (p.u.).
$P_{i_{\rm dc}j_{\rm dc}}$	DC power flow of dc cable $i_{\rm dc} - j_{\rm dc}$ (p.u.).
$P_{\rm loss}$	Total active losses of the whole system (p.u.).
$P_{\rm pcc}$	Active power at PCC bus (p.u.).
$Pr^{\rm yr.sn}$	Estimated power price within period p and year yr ($M/MWh).
$P_{vscloss}$	Total active losses of VSCs (p.u.).
PVF^{yr}	Present value factor of year (yr).
Q_c	Reactive power at VSC ac bus (p.u.).
Q_{gi}	Reactive power output from generator i (p.u.).
$Q_{\rm pcc}$	Reactive power at PCC bus (p.u.).
S_c	Apparent power at VSC ac bus (p.u.).
S_{ij}	Power flow of ac transmission line $i - j$ (p.u.).
TB	Total economic benefit [M$].
V_c	Voltage magnitude at VSC ac bus (p.u.).
$V_{\rm cdc}$	DC voltage at VSC dc bus (p.u.).
V_f	Voltage magnitude at VSC filter bus (p.u.).
V_i, V_j	Voltage magnitude at ac bus i and j (p.u.).
$V_{i_{\rm dc}}, V_{j_{\rm dc}}$	Voltage magnitude at dc bus $i_{\rm dc}$ and $j_{\rm dc}$ (p.u.).
$V_{\rm pcc}$	Voltage magnitude at PCC bus (p.u.).
δ_c	Voltage angle at VSC ac bus (degrees).
δ_f	Voltage angle at VSC filter bus (degrees).
δ_i, δ_j	Voltage angle at ac bus i and j (degrees).
$\delta_{\rm pcc}$	Voltage angle at PCC bus (degrees).

Indices:

i, j	Index of ac bus, generator, VSC station.
$i_{\rm dc}, j_{\rm dc}$	Index of dc bus.
p	Index of operation period.
yr	Index of year.

Sets:

N	Set of all ac buses.
NG	Set of all generators.
NL	Set of all loads.
M	Set of all dc buses.

Variable Limits:

$\underline{a}, \overline{a}$	Lower and upper limits of the variable a.

I. Introduction

A. Background and Motivation

THE electric power system is facing great challenges. The integration of large-scale renewable power resources increases the uncertainty of power generation. The interconnected electric power market requires more flexible power flow. The public pressure due to the environment impact of overhead transmission lines results in difficulties in the reinforcement of the aging transmission infrastructure system. High Voltage Direct Current transmission system based on Voltage Source Converter (VSC-HVDC) exhibits great positive potential in dealing with these challenges thanks to its specific performance characteristics [1]–[3], e.g., providing flexibility and controllability in managing real and reactive power flows, and possibility of using extruded XLPE dc cables. The multiterminal VSC-HVDC system (hereafter denoted as VSC-MTDC) can offer additional controllability in the transmission system to enable the system to be operated in an optimized way since it can affect the power flow of the connected ac grid across a much larger area compared to the two-terminal VSC-HVDC system.

To fully understand and evaluate the potential effect of VSC-MTDC on the steady-state operation, e.g., the reduction of power losses and generation cost, an optimal power-flow model (OPF) [4] of the mixed ac/dc grid, incorporating the VSC-MTDC system, is needed. Such an extended OPF model of a mixed ac/dc transmission system (denoted in this paper as the M-OPF) plays an important role in determining the potential operational benefit in the planning process when considering VSC-MTDC as reinforcement candidates. It is also indispensable for the optimal operation of the electric power system.

Towards this end, several research works have been carried out proposing models and methods for inclusion of a VSC-MTDC system into the power-flow calculation of a mixed ac/dc transmission system. A unified method to calculate the load flow of a mixed ac/dc grid has been proposed in [5]. However, the VSC station (including VSC, phase reactors, and ac filter, and excluding the transformer) was modeled as a voltage source in [5], which did not present a general configuration of a VSC station, and is not capable of reflecting the influence of station equipment (e.g., an ac filter) on the actual power flow. A more detailed VSC model on the basis of the general configuration of a VSC station was introduced in [6] and [7] for the power-flow calculation of a mixed ac/dc grid. However, the OPF model was not considered in these two studies. An OPF model incorporating a VSC-HVDC system was introduced in [8] and the VSC-HVDC system introduced in the paper is limited to a two-terminal configuration. OPF models incorporating a VSC-MTDC system were proposed in [9] and [10]. The VSC (converter itself) was modeled as a power source connecting the ac and dc grid in these two papers. However, the OPF model in [9] only included the power relationship between the ac and dc sides of a VSC; the voltage relationship was not considered. In [10], the whole VSC station is modeled as a power source, which is similar to the method shown in [5]. Therefore, the influence of station equipment (e.g., an ac filter) on the actual power flow cannot be reflected either.

When the VSC-MTDC system is considered for network reinforcement of an ac transmission system, the economic assessment of a proposed VSC-MTDC system will be one of the most important tasks during the overall transmission planning phase. Before deregulation, the electric power system was vertically integrated and centrally managed. The decision on expansion projects was based on the investment and operation cost minimization principle [11]. In a deregulated electricity market, the transmission planning is driven by market based initiatives, and the target of the transmission expansion focuses on the maximum social welfare, e.g., increasing transmission capacity to allow the most efficient use of generation [12]. Numerous studies focusing on the various aspects of the transmission expansion planning in a competitive electricity market were proposed [12]–[14], e.g., simulating the electricity market, modeling the electric power system, defining the objective functions, etc. The transmission expansion planning process and methodologies commonly used nowadays in practices is introduced in [12] and [15]. The whole planning process is identified as a multi-objective task with consideration of uncertainties and risk situations, and the cost-benefit analysis for the economic assessment of alternatives is generally used during the planning process [12].

Most of studies listed and reviewed in [12]–[15] focused on the ac alternatives in the system reinforcement, only a few papers were found considering HVDC systems, especially the VSC-MTDC systems, as candidates. The economic assessment of the VSC-HVDC connection of offshore wind farms, compared to ac alternatives, was presented in [16]. The cost of investment, operation and maintenance, and power losses of both ac and dc alternatives were compared and the break-even point of ac versus dc transmission was analyzed. The economic evaluation of an embedded HVDC system in an ac grid was presented in [17] and [18]. The economic benefit of HVDC project was analyzed on the basis of a market simulation in [17]. The benefit was defined as the sum of consumer, producer, and transmission surpluses. In contrast, an economic evaluation of the HVDC focusing on the cost minimizing was presented in [18]. The investment and maintenance cost as well as the cost of power losses were considered. However, the HVDC systems (VSC or LCC HVDC) in these papers were limited to the two-terminal configuration. A hybrid ac/dc transmission expansion planning model was proposed in [19] to minimize the total investment, operation and load shedding costs. However, the dc network was represented as a simple model neglecting the dc power-flow equations.

When a meshed dc grid, such as a VSC-MTDC system, is embedded into an ac grid, its influence to the system overall power flow is much complicated than HVDC links integrating offshore wind farms or two-terminal HVDC systems in an ac grid. Therefore, the benefit from using embedded VSC-MTDC system should be evaluated from the perspective of the whole mixed ac/dc system, such as the benefit from reducing the total generation cost and system power losses. Meanwhile, the investment cost of a VSC-MTDC system, is much higher than the cost of corresponding ac alternatives. Therefore, the proper economic assessment of the HVDC system should include both benefit analysis and cost comparison, which is the main reason that the cost-benefit analysis is used for the economic assessment of VSC-MTDC systems in this paper.

B. Objectives and Main Contributions of the Study

The main objectives of this paper are to propose a Mixed ac/dc OPF model (M-OPF) to incorporate the VSC-MTDC system with a general configuration which can be used for the operation and planning purposes of the ac transmission system with an embedded VSC-MTDC system. In this study, the proposed M-OPF model is used as a *calculation engine* in a cost-benefit analysis approach for the economic evaluation of the embedded VSC-MTDC systems compared to other dc and corresponding ac alternatives during the transmission expansion planning process when VSC-MTDC systems are considered as candidates. In this approach, the operational benefits of the VSC-MTDC systems are evaluated against their investment costs to derive the Benefit-to-Cost Ratios (BCR). Thus, the configuration and location of the preferred alternative of VSC-MTDC systems can be suggested based on the BCR values.

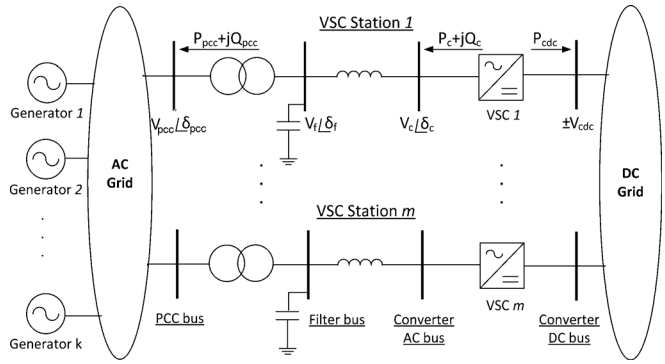

Fig. 1. The ac grid with an embedded VSC-MTDC system and the general configuration of the VSC station.

C. Organization of the Paper

The paper is organized as follows: In Section II, the modeling of the VSC-MTDC in the OPF is presented. Section III describes the proposed formulation of the M-OPF model. Section IV presents the proposed cost-benefit analysis approach using the proposed M-OPF model. The results and discussions of the case study using the M-OPF model and cost-benefit approach are presented in Section V. Finally, the conclusions of this study are presented in Section VI.

II. Modeling of VSC-MTDC in an Optimal Power-Flow Framework

A general mixed ac/dc system with VSC stations is depicted in Fig. 1. It should be noted that the VSC refers to the voltage source converter itself in this paper, and the VSC station includes VSC and other equipments, e.g., phase reactors, filters, and transformers. As can be seen, the mixed ac/dc system consists of two major parts: the meshed ac grid and dc grid which are connected by VSC stations at some buses. The ac network may represent ac buses, transmission lines, transformers, shunt capacitors/reactors, etc. The dc grid includes dc buses, dc cables or overhead lines, etc. The dc generations, dc loads and dc/dc converters used to transfer dc voltages to different levels may also be included in the dc network; however, they are not considered in this paper. The configuration of the VSC station shown in Fig. 1 refers to the traditional two- or three-level converter with the Pulse-Width Modulation switching method (PWM). When the Modular Multi-level Converter (MMC) using the cascade connection modulation method is used, ac filters can be omitted [20].

The basic operation principle of the VSC station is widely familiar. By appropriately modulating the magnitude and phase angle of the voltage at the VSC ac terminal, the ac current through the phase reactor can be regulated. Thus, the active and reactive power at the Point of Common Coupling (PCC) bus can be controlled [1]. With different control strategies, the voltage and even frequency at the PCC bus can be controlled as well [21].

A. Review of Normal Power-Flow Calculation of the Mixed AC/DC Grid

The conventional ac power-flow calculation method uses active and reactive power injections from generators as known quantities to calculate variables, e.g., bus voltages and angles. When the VSC is considered as a power source, its active and reactive power outputs are also known quantities in the power-flow equations [5]. The same concept is applied to the power-flow calculation of a meshed dc grid. The dc power injection from VSC, i.e., $\mathrm{P_{cdc}}$ (as shown in Fig. 1), is used as a known quantity to calculate the dc bus voltages. If the VSC is treated as a lossless power exchanger, the dc power injection, $\mathrm{P_{cdc}}$, will have the same magnitude but opposite direction of the ac power injection (i.e., $\mathrm{P_c}$). Therefore, the key point of solving the power-flow equations of the dc grid is to find the ac power injection (i.e., $\mathrm{P_c}$) from the ac side. However, since the active and reactive power outputs of the VSC station are regulated at the PCC bus as described above, the power at the PCC bus (i.e., $\mathrm{P_{pcc}}$ and $\mathrm{Q_{pcc}}$) are known, while the power at the VSC ac terminal (i.e., $\mathrm{P_c}$ and $\mathrm{Q_c}$) are unknown in the power-flow calculation. Therefore, in order to solve the power-flow equations of a meshed dc grid, the ac power (i.e., $\mathrm{P_c}$) has to be first calculated on the basis of the controlled ac power at PCC bus (i.e., $\mathrm{P_{pcc}}$ and $\mathrm{Q_{pcc}}$) and the initial bus voltages or the bus voltages from the previous step of the iterative loop when the Newton-Raphson method is used. This is described in [6] as a step of a sequential method. This calculation step would increase the complexity of computation when it is included in the OPF model, and might lead to difficulties in obtaining the solutions from the OPF model.

B. Treatment of VSC-MTDC in the M-OPF Model

In the OPF calculation method, the controlled power injections from generators and VSC stations to ac or dc grids are considered as the control (optimization) variables. By selecting the optimal values of these variables, a certain operational objective of the mixed ac/dc transmission system can be achieved. When a certain power-flow solution is settled and if the transformer ratio is fixed, the optimal solution at the PCC bus (i.e., $\mathrm{P_{pcc}}$, $\mathrm{Q_{pcc}}$, $\mathrm{V_{pcc}}$, and δ_{pcc}) will have only one corresponding optimal solution on the converter ac bus (i.e., $\mathrm{P_c}$, $\mathrm{Q_c}$, $\mathrm{V_c}$, and δ_{c}). Therefore, the active and reactive powers flowing from the VSC to the converter ac bus (i.e., $\mathrm{P_c}$ and $\mathrm{Q_c}$) can be used as the control variables in the M-OPF model, instead of the active and reactive power injections at the PCC bus (i.e., $\mathrm{P_{pcc}}$ and $\mathrm{Q_{pcc}}$). This yields the fact that pre-calculating the power flow from the PCC bus to the converter ac bus would be unnecessary compared to the sequential method describe above, and consequently reduce the calculation effort.

Thus, the proposed basic approach of incorporating the VSC-MTDC system into the conventional ac grid in the M-OPF model may be described as follows:

- VSCs work as power sources injecting ac and dc power into two sides separately. If the power loss of the VSC were neglected, the injected ac and dc active power from VSCs have same magnitudes but with opposite directions.
- The power injections from VSCs to the ac and dc grid are limited by constraints from both the ac and dc sides, including maximum bus voltage limits, maximum valve current limit, etc.
- The power-flow equations of the ac and dc grid are coupled by the active power exchange through VSCs. They can

be used directly and solved simultaneously in the M-OPF model.

C. Mathematic Model of the VSC Station

The VSC station is modeled in steady state according to the proposed approach described above. The VSC station model includes two parts: 1) the power and voltage relationships between ac and dc sides; 2) VSC capacity constraints.

1) Power and Voltage Relationships in AC/DC Grids: As discussed above, the VSC is considered as an electric power exchanger. When power losses are neglected, the power exchange of the VSC is defined in (1)

$$P_c = -P_{\mathrm{cdc}}. \tag{1}$$

In order to avoid the harmonics because of the over-modulation of the VSC, the peak value of the phase voltage at the converter ac bus is assumed to be lower than the corresponding converter dc bus voltage in this paper as suggested in [22]. Thus, the voltage relationship between ac and dc bus of the VSC can be defined using real values as shown in (2)

$$\bar{V}_c = (\frac{\sqrt{3}}{\sqrt{2}})V_{\mathrm{cdc}}. \tag{2}$$

Equation (2) can be re-written in the per unit form as expressed in (3), where the voltage relationship factor $(\mathrm{k_v})$ is defined by the allowed maximum ac bus voltage

$$\bar{V}_c = k_v V_{\mathrm{cdc}}. \tag{3}$$

In this paper, the nominal dc and ac voltages are both set at 1 p.u., and the maximum ac bus voltage is assumed to be 1.1 times of the nominal ac bus voltage. Thus, $\mathrm{k_v}$ is set to 1.1 in this paper. If the over-modulation mode or other methods are used for the purpose of obtaining higher voltage at the VSC ac bus, factor $\mathrm{k_v}$ can be modified according to the requirement. However, these special cases are not considered in this study. The voltage at the VSC ac bus is limited by (4)

$$V_c \le \bar{V}c. \tag{4}$$

2) The VSC Capacity Constraints: The normal operation of the VSC is principally constrained by the maximum current through VSC valves and the maximum dc voltage [3]. The former determines the maximum VSC apparent power limit, and the latter defines the VSC reactive power output limit. Usually, VSC constraints are applied at the PCC bus [6]. In this OPF model, VSC constraints at the converter ac bus are used because the VSC power exchange at the converter ac bus is set as control variables.

Maximum Apparent Power Constraint: Given the maximum valve current, the apparent power of VSC can be defined in (5)

$$|S_c| \le |V_c \bar{I}_v|. \tag{5}$$

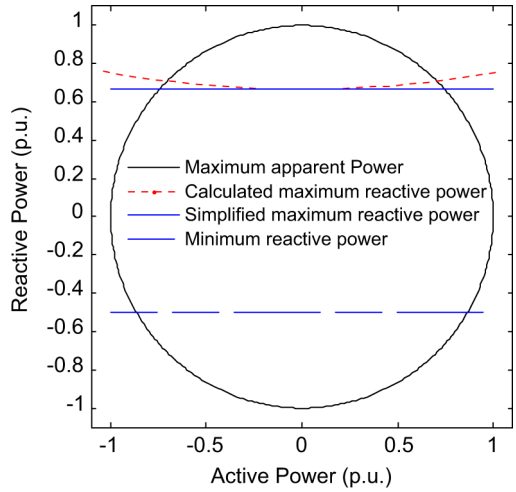

Fig. 2. Example of the VSC power capacity curves ($\bar{I}_v = 1$ p.u., $\mathrm{Vc} = 1$ p.u., $\mathrm{Vf} = 0.9$ p.u., $\mathrm{Rr} = 0.0001$ p.u., and $\mathrm{Xr} = 0.15$ p.u.).

Equation (5) can also be rewritten as in (6)

$$P_c^2 + Q_c^2 \le (V_c \bar{I}_v)^2. \tag{6}$$

The apparent power range on the VSC power plane defined by (6) can be plotted as shown in Fig. 2.

Maximum Reactive Power Constraint: The maximum reactive power constraint of the VSC is defined in (7), assuming that the conductance of the phase reactor is much smaller than its susceptance.

$$\bar{Q}_c = -B_r(\bar{V}_c^2 - \bar{V}_c V_f e^{j(\delta_c - \delta_f)}). \tag{7}$$

As can be seen in Fig. 2, the reactive power variation (the dotted red curve) inside the black circle is quite small compared to the nominal VSC rating (about 3% of the nominal VSC rating in this case). To simplify the calculation, the maximum reactive power output limit is set as the minimum value of the red curve when $\delta_c - \delta_f = 0$, which is defined in (8). The new maximum reactive power limit is shown by the solid line in Fig. 2

$$\bar{Q}_c = -B_r(\bar{V}_c^2 - \bar{V}_c V_f). \tag{8}$$

Minimum Reactive Power Constraint: The minimum reactive power constraint of the VSC is expressed by (9). This limit depends on the specific requirement of each project. In this study, to simplify the model, it is assumed as a fixed value as shown by the dashed blue line in Fig. 2. The constraint factor $(\mathrm{k_Q})$ is decided by the design of the real project

$$\underline{Q}_c = -k_Q S_{\mathrm{nom}}. \tag{9}$$

III. Mathematical Formulation of the Mixed AC/DC OPF Model (M-OPF)

This section presents the objective functions and constraints of the proposed mixed ac/dc OPF model referred to as M-OPF. It shall be clarified that the variables used in the equations of

Section II will be specified with indices in this section. For example, $\mathrm{P_c}$ in (1) will be presented as $\mathrm{P_{ci}}$ in (16), which indicates the power injection to the bus i.

A. Objective Functions

1) Minimization of Total Generating Cost: The first objective function considered in the M-OPF model is the total generation cost which will be minimized as shown

$$\text{Minimize Cost} = \sum_{i=1}^{\mathrm{NG}} (A_{ci} + B_{ci} Pgi + C_{ci} P_{gi}^2). \tag{10}$$

2) Minimization of Total Transmission Loss: The second objective function considered in the M-OPF model is the total active power loss of the mixed ac/dc system which will be minimized as shown

$$\text{Minimize } P_{\mathrm{loss}} = P_{\mathrm{acloss}} + P_{\mathrm{dcloss}} + P_{\mathrm{vscloss}}. \tag{11}$$

The total active power loss includes three components: active power loss of the ac transmission lines, active power loss on dc cables, and active power losses of VSCs, as follows.

- Active power loss of the ac transmission lines can be calculated using [23] as follows:

$$P_{\mathrm{acloss}} = 0.5 \sum_{i=1}^{N} \sum_{j=1}^{N} g_{ij} (V_i^2 + V_j^2 - 2V_i V_j \cos(\delta_i - \delta_j)). \tag{12}$$

- Active power loss on dc cables can be calculated using

$$P_{\mathrm{dcloss}} = 0.5 \sum_{i_{\mathrm{dc}}=1}^{M} \sum_{j_{\mathrm{dc}}=1}^{M} g_{i_{\mathrm{dc}} j_{\mathrm{dc}}} (V_{i_{\mathrm{dc}}} - V_{j_{\mathrm{dc}}})^2. \tag{13}$$

- Active power loss of VSCs can be expressed as a quadratic function of the phase current of VSC valves as shown in (14)[24]:

$$P_{\mathrm{vscloss}} = \sum_{i=1}^{M} (A_{li} + B_{li} I_{vi} + C_{li} I_{vi}^2) \tag{14}$$

where the phase current of VSC valves can be calculated using

$$(I_{vi} V_{ci})^2 = {P_{ci}}^2 + {Q_{ci}}^2 \quad \forall i \epsilon M. \tag{15}$$

B. Constraints

The two objective functions described before are subjected separately to the same set of technical constraints.

1) Constraints From the AC System [4]:

- AC load-flow equations:
  The load-flow equations of the ac grid are modified by incorporating the active power injections from VSCs and the VSC losses as shown

$$P_{gi} + P_{ci} - P_{di} - P_{\mathrm{vsclossi}} = V_i \sum_{j=1}^{N} (G_{ij} \cos(\delta_i - \delta_j) + B_{ij} \sin(\delta_i - \delta_j)) V_j \quad \forall i \in N \tag{16}$$

$$Q_{gi} + Q_{ci} - Q_{di} = V_i \sum_{j=1}^{N} [G_{ij} \sin(\delta_i - \delta_j) - B_{ij} \cos(\delta_i - \delta_j)] V_j \quad \forall i \in N. \tag{17}$$

- Generator active and reactive power limits

$$\underline{\mathrm{P}}_{gi} \le \mathrm{P}_{gi} \le \bar{\mathrm{P}}_{gi} \quad \forall i \epsilon \mathrm{NG} \tag{18}$$

$$\underline{\mathrm{Q}}_{gi} \le \mathrm{Q}_{gi} \le \bar{\mathrm{Q}}_{gi} \quad \forall i \epsilon \mathrm{NG}. \tag{19}$$

- AC bus voltage limits

$$\underline{V}_i \le V_i \le \bar{V}_i \quad \forall i \epsilon \mathrm{N}. \tag{20}$$

- AC transmission line capacity limit:

$$\underline{S}_{ij} \le S_{ij} \le \bar{S}_{ij} \quad \forall i \epsilon N, \forall j \epsilon N. \tag{21}$$

2) Constraints From the VSC-MTDC System [5], [6]:

- The dc load-flow equations:
  The balanced bipolar VSC configuration is considered to be the normal operation mode in this study. The dc load-flow equations of this configuration may be expressed in the following way:

$$P_{i_{\mathrm{dc}}} = 2V_{i_{\mathrm{dc}}} \sum_{j_{\mathrm{dc}}=1}^{M} G_{i_{\mathrm{dc}} j_{\mathrm{dc}}} V j_{\mathrm{dc}} \quad \forall i_{\mathrm{dc}} \epsilon M. \tag{22}$$

- The dc bus voltage limits

$$\underline{V}_{i_{\mathrm{dc}}} \le V_{i_{\mathrm{dc}}} \le \bar{V}_{i_{\mathrm{dc}}} \quad \forall i_{\mathrm{dc}} \, \epsilon M. \tag{23}$$

- The dc transmission-line flow limits

$$\underline{P}_{i_{\mathrm{dc}} j_{\mathrm{dc}}} \le P_{i_{\mathrm{dc}} j_{\mathrm{dc}}} \le \bar{P}_{i_{\mathrm{dc}} j_{\mathrm{dc}}} \quad \forall i_{\mathrm{dc}} \, \epsilon M, \forall j_{\mathrm{dc}} \, \epsilon M. \tag{24}$$

3) Constraints on VSC: Specific constraints of the VSC model were previously introduced in Section III. Equations (1), (3), (4), (6), (8), and (9) are included in the M-OPF model.

C. Comments on the Solution Method

The proposed M-OPF model is a nonlinear optimization problem. It is implemented using a general algebraic modeling system (GAMS) [25], and is solved with a nonlinear solver IPOPT [26]. MATLAB is employed in the data preparation and results processing.

It should be noted that the nonlinear optimization problem could have solutions based on local optimums. The IPOPT solver uses an "interior point line search filter" method [26] and is commonly used in solving large-scale nonlinear optimization problems. In the study, different popularly used solvers, including MINOS, CONOPT, and IPOPT, are tried to solve the M-OPF model. The IPOPT solver gives the best results

compared to the results obtained from other solvers. The default value of the relative convergence tolerance of the algorithm of 10^{-8} of IPOPT is used. In this paper, the focus is on the formulation of the M-OPF model rather than on the development of the advanced solution algorithms for the global optimum of the nonlinear optimization problem. For different (local optimal) solutions with the same objective function value, the total benefits obtained based on local optimums could be the same; however, the generation dispatches and system losses could be different. The focus of the analysis in this paper is on the total benefits to evaluate the economics of VSC MTDC alternatives which are therefore not affected by this issue.

IV. Cost-Benefit Analysis for the Evaluation of VSC-MTDC Systems

In this section, a cost-benefit analysis approach to evaluate the costs and benefits of the VSC-MTDC systems over a period of time is proposed using the M-OPF model described in Section III. The approach will use the BCR, an indicator of cost-effectiveness of the projects, to rank the alternatives of the VSC-MTDC systems according to their economic performance in the case study which will be described in Section V.

The total economic benefit due to the VSC-MTDC system is defined as the sum of the reduction of the system generation cost and the reduction of the cost of the active power losses of the system compared to the case without the deployment of the VSC-MTDC system. The present value of the total economic benefit is calculated for a period of 30 years using (25). The annual system load growth is assumed to be 0.5% over a period of 30 years. Each year is divided into four equal periods. The load coefficients of four periods are calculated based on typical peak load values for each period in Sweden in 2011 [27] and are provided in Table II. The coefficients of these periods are used to calculate the load level in each period per year

$$\mathrm{TB} = \sum_{yr=1}^{30} (\mathrm{PVF}^{\mathrm{yr}} \sum_{p=1}^{4} (t(c_1^{\mathrm{yr}\cdot p} - c_2^{\mathrm{yr}\cdot p}) + \mathrm{pr}^{\mathrm{yr}\cdot p}\, t(L_1^{\mathrm{yr}\cdot p} - L_2^{\mathrm{yr}\cdot p}))) \quad (25)$$

$$\mathrm{PVF}^{\mathrm{yr}} = \frac{1}{(1+r)^{\mathrm{yr}-1}}. \quad (26)$$

The discount rate used in this study is assumed to be 8%. The selection of the discount rate is a rather complex issue involving the weighted average cost of capital and the risks of the projects. The lower discount rate (e.g., 5% as suggested in [28]) would often be chosen for the low-risk project (could be smaller investment) while the higher discount rate (e.g., 10% as suggested in [28]) would be chosen for the high-risk project (could be larger investment). It is needless to say that the change in the value of the discount rate would affect the discounted total benefit/cost of the project. For example, a higher discount rate would imply lower total discounted benefits of the project which accounts for the higher risks project. The selected discount rate used in this paper is somewhere in between. It would be interesting to see the effects of the changes in the outcomes of the analysis, that is, on the benefits and costs of the alternative projects. This is, however, not in the scope of this paper.

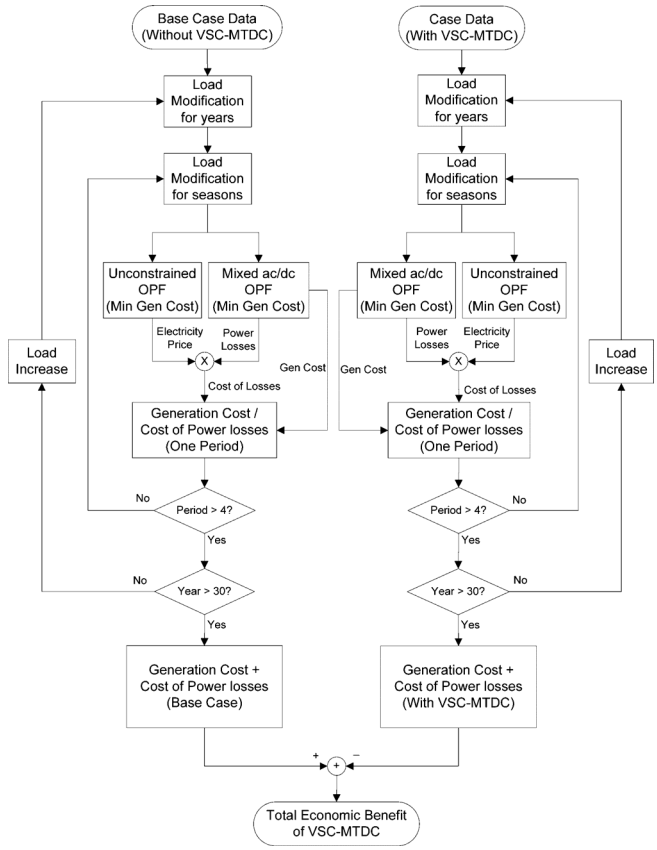

Fig. 3. Proposed approach for the total economic benefit calculation.

The power price is estimated using unconstrained OPF [23] on the basis of the modified system load at season p and year *yr*. The objective of this unconstrained OPF is to minimize the generation cost.

The calculation process for the total economic benefit is shown in Fig. 3.

In the calculation, for each of the candidate VSC-MTDC systems, the M-OPF model is executed with the objective function (10), that is, the minimization of the total system cost for the base case and for the case with the selected VSC-MTDC system. Each model run provides the total generation costs and total system losses simultaneously for the cases considered. The total loss is converted to the cost of total loss by multiplying the power price calculated using the same M-OPF model run but without the transmission constraints (unconstrained case). It has been assumed that the compensated power due to losses has to be purchased at the unconstrained market price. The difference between the total costs in the two cases with and without VSC-MTDC represents the economic benefits of each alternative considered. The BCR as expressed in (27) is calculated for each of the candidate VSC-MTDC systems

$$\mathrm{BCR} = \frac{\mathrm{TB}}{\mathrm{Inv}}. \quad (27)$$

The investment cost of the VSC-MTDC system, including the cost of VSC station equipment and dc cables for each case, is estimated by linearly scaling the investment of one project presented in [29] and shown in Table III. The maintenance cost of VSC-MTDC is not taken into account.

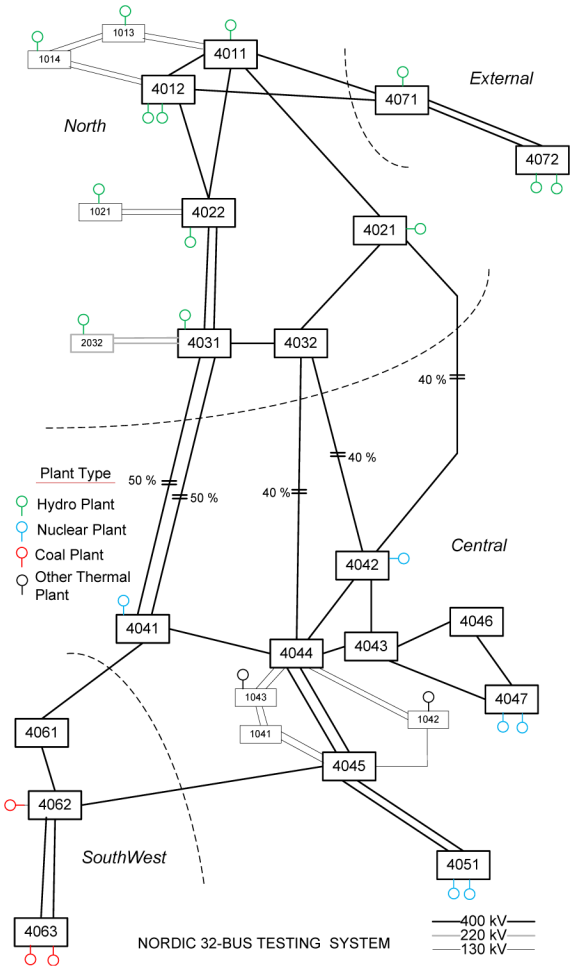

Fig. 4. Network topology of the Nordic 32-bus system.

TABLE I
VSC-MTDC SYSTEMS FOR THE CASE STUDY

Case Number	VSC Location (Connected ac bus)	Number of VSC stations	Topology Type [1]
Base Case	Nordic 32-bus system		
Case-1	4032 – 4044[2]	2	
Case-2	4021 – 4032 – 4044	3	Serial
Case-3	4021 – 4032 – 4031, 4032 – 4044	4	Radial
Case-4	4011 – 4021 – 4032 – 4044	4	Serial
Case-5	4022 – 4031 – 4041	3	Serial
Case-6	4012 – 4022 – 4031 – 4041	4	Serial
Case-7	4022 – 4031 – 4032, 4031 – 4041	4	Radial
Case-8	4011 – 4022 – 4031 – 4041	4	Serial
Case-9	4031 – 4041 – 4044	3	Serial
Case-10	4031 – 4032 – 4044	3	Serial
Case-11	4022 – 4031 – 4032 – 4044	4	Serial
Case-12	4021 – 4032 – 4042 – 4021	3	Ring
Case-13	4032 – 4042 – 4044 – 4032	3	Ring
Case-14	4044 – 4045 – 4051	3	Serial
Case-15	4032 – 4044 – 4045	3	Serial

[1] "Topology Type" indicates the configuration of VSC-MTDC systems. "Serial" means that all VSC stations are connected by dc cables one by one as a string; "Radial" means that VSC stations are connected by dc cables in a star configuration; "Ring" means that VSC stations are connected by dc cables in a close loop. Fig. 5 shows the typical topologies of VSC-MTDC systems.
[2] The bus numbers indicates the ac buses which are connected to the corresponding VSC stations. In addition, one ac transmission line between two buses is replaced by the corresponding dc cable.

V. CASE STUDY: RESULTS AND DISCUSSIONS

A. Description of the Studied System

1) Nordic 32-Bus System and Assumption: The Nordic 32-bus system is a benchmark grid representing the fundamental features of the Swedish HV transmission system [30]. The single-line diagram of the system is shown in Fig. 4.

All generators of the Nordic 32-bus system are classified into four types: hydroplants, nuclear plants, coal thermal plants, and others. The generation cost coefficient data in the system are not available. In this study, the cost coefficients for each type of generation are estimated by using the typical values provided in [31]. The values calculated were calibrated using the generation costs of different types in the Nordic countries for 2003 [32]. Finally, they were further adjusted so that the calculated unconstrained market price would be in the current market price range for the Nordic day-ahead market [27]. The calculated cost coefficients for all system generators are provided in Table IV.

Definition of the Study Cases: A total of 16 study cases corresponding to the base case (i.e., the original Nordic 32-bus system without any VSC-MTDC system) and another 15 cases representing cases with different VSC-MTDC configurations were considered in the study. The dc cables of the VSC-MTDC system are in each case used to replace corresponding ac transmission lines. The motivation behind the definition of these cases is to increase transmission system capability, or replace the ac transmission lines with high losses by dc cables. With the VSC-MTDC system embedded, the transmission system is expected to transfer more hydro power from the North to the South in the system and/or some heavily loaded ac transmission lines could be relieved. Thus, the total generation cost or system power losses could be reduced. Table I lists all considered cases. In all study cases, it is assumed that the number of terminals of the VSC-MTDC system is limited to four, and the VSC stations are assumed to be identical. The configuration of VSC stations is shown in Fig. 1, and the parameters of the VSC station used in the study are listed in Table V.

The converter transformer is assumed to have a fixed turns-ratio. The VSC power loss at the nominal condition is assumed to be 1.76% of the nominal VSC rating as suggested in [24]. When the new generation of VSC is used, the VSC loss value can be reduced to 0.9% or even further reduced to 0.5% for the MMC [33]. The effects of the lower loss values of VSC to the total benefit are tested by means of sensitivity analyses described in Section V-B3. The loss coefficients of the VSC station are derived from the "South West Link" HVDC project in Sweden [24], and are scaled to fit the VSC rating. The total power losses of all VSCs are determined by (14). The topologies of the selected VSC-MTDC systems are shown in Fig. 5.

The type of dc cable is selected from [34] according to the VSC rating. A land cable with the aluminum conductor area of 2000 mm^2 is used. In order to obtain the lumped resistance of each dc cable, the length of the corresponding ac transmission line is estimated based on the resistance of the line and the general unit resistance. Thereafter, using the same length of ac transmission line, the lumped resistance of the dc cable is calculated.

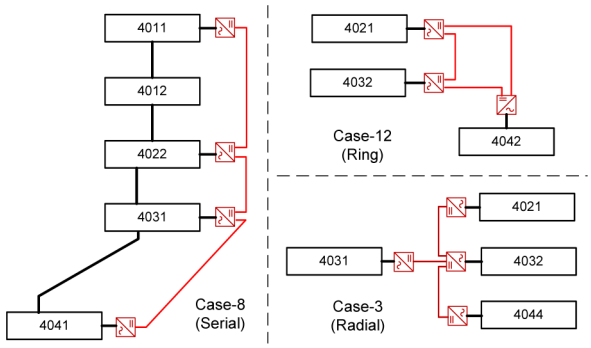

Fig. 5. Configuration of VSC-MTDC systems: Case-3, Case-8, and Case-12.

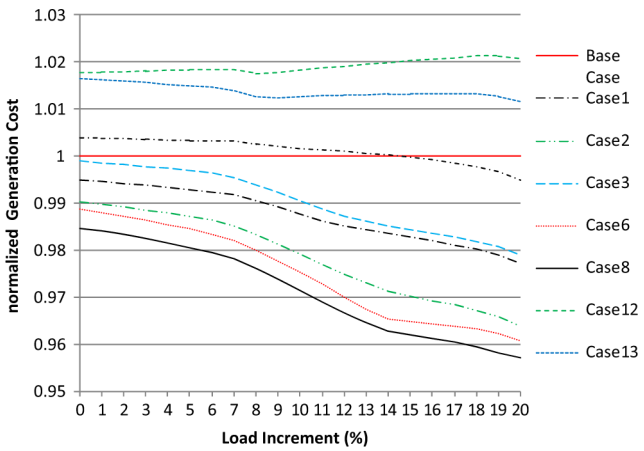

Fig. 6. Normalized generation cost of 15 cases under different load conditions. The objective of M-OPF is to minimize the generation cost.

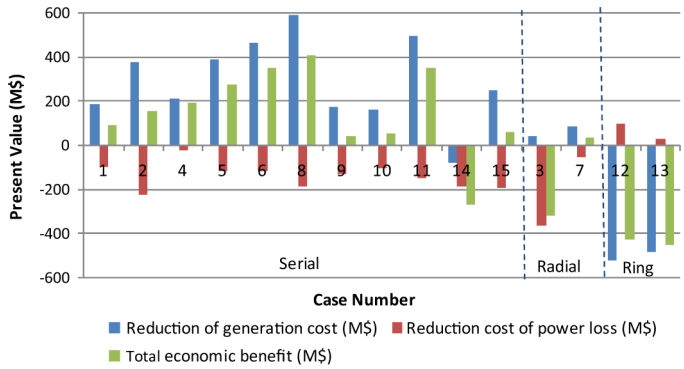

Fig. 7. Present value of the reduction of generation cost, the reduction of costs of power loss, and the total economic benefit. The results are grouped based on the topology type of VSC-MTDC systems (as shown in Table I). The objective of M-OPF is to minimize the generation cost.

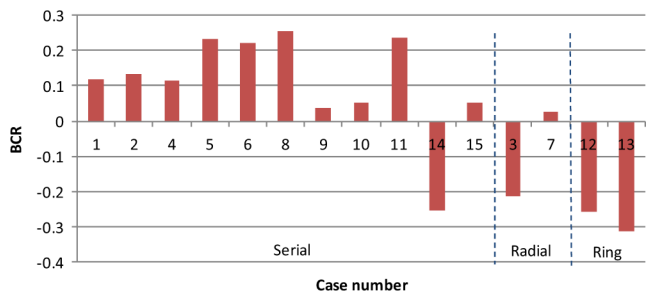

Fig. 8. BCRs of VSC-MTDC systems. The results are grouped based on the topology type of VSC-MTDC systems (as shown in Table I).

B. Cost-Benefit Analysis of VSC-MTDC Systems

1) Evaluation of Generation Cost Reduction Due to VSC-MTDC Systems: As a first step of the cost-benefit analysis, the M-OPF model is executed with the objective function of minimizing the total generation cost. In order to understand the economic benefits of the VSC-MTDC under different system conditions, the transmission system is incrementally stressed by increasing the system load. The system load is increased equally at all load busses in steps of 1% of the nominal value up to 120%. Fig. 6 shows the generation cost of the selected 15 cases. The costs are normalized over the base case (pure ac system) for the same load condition. As can be seen in the figure, in most cases (except Case-12 and Case-13), the generation costs are reduced by using VSC-MTDC.

2) Cost-Benefit Analysis: the Benefit-to-Cost Ratios (BCRs): The cost-benefit analysis for the alternatives of the VSC-MTDC system has been carried out using the approach described in Section IV. The calculated total benefits (i.e., the sum of reduction in generation cost and reduction of active power loss cost) of all the considered cases are shown in Fig. 7

It is noted that the results are calculated for 30 years. As can be seen in Fig. 7, 11 out of 15 cases considered have shown positive total benefits from using VSC-MTDC systems. The cases with high total benefits correspond to the "serial" topology type of VSC-MTDC, while all of the cases using the radial or ring topology of the VSC-MTDC system show much smaller or even negative benefits. This could be due to the fact that the same rating is used for all VSC stations. When two dc links are connected to one VSC station in the cases using radial or ring topology type, they are limited by the capacity of that VSC station. Therefore, the capacity of these two dc links cannot be fully utilized. Case-8 appears to have the highest total benefit because it has the highest reduction in total generation cost, even though it has the negative reduction cost of power loss (i.e., increase in the cost of loss). This might be attributed to the fact that the VSC-MTDC system in Case-8 connects the generation area in the North with the load area in the South. The configuration and connection of the VSC-MTDC system in Case-8 are shown in Fig. 5. Since the power flow through the dc links in this case is controlled at their highest capacities, the total power transmission from North to South is increased compared to that in the base case with only ac transmission lines. Therefore, the total generation cost is reduced because more hydropower generation can be used. On the other hand, the VSC introduces more power loss with the transmission of high power. Therefore, the total system power loss in this case is more than that of the base case.

Fig. 8 shows the calculated BCRs for all cases. The BCRs reflect the economic performance of the alternatives considered in terms of system cost reduction for every dollar of investment cost. From the figure, it can be seen that Case-8 has the highest BCR which is the preferred case from an economic benefits perspective. Case-5, Case-6, and Case-11 are among the other cases with high BCRs. However, the BCRs for all cases are found to be lower than unity and some of them are even negative, which

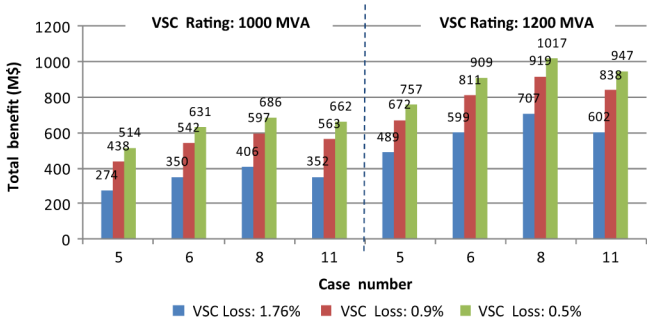

Fig. 9. Changes in the total benefit when VSC capacity and losses are changed.

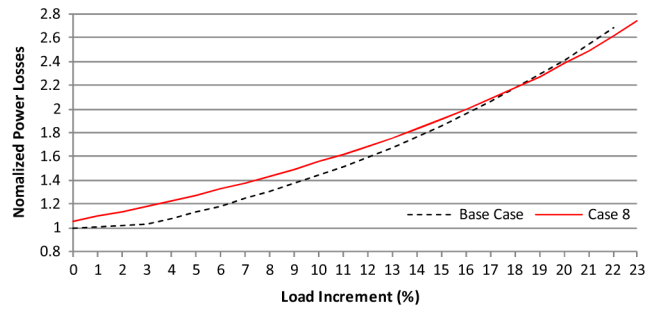

Fig. 10. Normalized power losses of Case-8 in different load conditions over the base case.

TABLE II
LOAD COEFFICIENTS (*)

Period	Jan - Mar	Apr - Jun	Jul - Aug	Oct - Dec
Coefficient	1.00	0.76	0.64	0.84

(*) The coefficients are calculated based on data from [27].

TABLE III
UNIT COST OF THE VSC STATION AND DC CABLE [29].

Item	Unit	Cost	Device Parameter
VSC station	1 station	283 M$	1000 MVA, ±300 kV
HVDC Cable	1 km	0.7 M$	Land cable, 2000 mm^2, ±300 kV

means the total benefits considered in this study by utilizing VSC-MTDC are lower than its investment cost. It should be noted that this study focuses on analyses in the steady state. The other technical benefits in the dynamic state, including the improvement of system controllability and dynamic performance, are beyond the scope of the present study. In addition, the transmission charge could be considered a source of income from the project. It will be studied in the future work, and has not been included in this study. If such benefits could be considered, the BCRs would obviously be much higher. Therefore, BCR is only one of the "performance indicators" which should be considered in selecting VSC-MTDC projects.

3) Sensitivity Analyses: VSC Nominal Capacity and VSC Loss Level: In order to understand how the results (i.e., the BCRs values) would vary with changes in the technologies of VSC-MTDC systems, sensitivity analyses have been performed with regard to the changes in nominal capacity and VSC losses for four selected Cases-5, 6, 8, and 11. Summary results of

TABLE IV
CALCULATED GENERATOR COST COEFFICIENTS.

Bus	Ac ($)	Bc ($/MWh)	Cc ($/MW^{2}h)	Plant Type
1012	809	15.4	0.0026	Hydro
1013	1079	20.5	0.0026	Hydro
1014	925	17.6	0.0026	Hydro
1021	1076	20.5	0.0026	Hydro
1022	1619	30.8	0.0026	Hydro
1042	2226	49.2	0.0225	Other thermal
1043	2477	54.8	0.0225	Other thermal
2032	809	15.4	0.0026	Hydro
4011	647	12.3	0.0026	Hydro
4012	809	15.4	0.0026	Hydro
4021	1439	24.7	0.0026	Hydro
4031	1349	25.7	0.0026	Hydro
4042	2070	40.9	0.0048	Nuclear
4047	2229	44.0	0.0048	Nuclear
4047	2229	44.0	0.0048	Nuclear
4051	2070	40.9	0.0048	Nuclear
4051	2070	40.9	0.0048	Nuclear
4062	3264	72.2	0.0297	Coal fired
4063	3264	72.2	0.0297	Coal fired
4063	3264	72.2	0.0297	Coal fired
4071	1076	20.5	0.0026	Hydro
4072	809	15.4	0.0026	Hydro

the sensitivity analyses are shown in Fig. 9. As can be seen in the figure, when the capacity of the VSC-MTDC system is increased by 20%, from 1000 MW to 1200 MW (the dc cable conductor area is changed to 2200 mm^2), the total benefits for all four cases are increased by about 70% when the VSC loss is 1.76% of the nominal VSC capacity, and by about 50% when the VSC loss is 0.9% or 0.5% of the nominal VSC capacity. When VSC losses are decreased to 0.9% of the nominal VSC capacity, the total benefits for all four cases above are increased by about 50% for the VSC capacity of 1000 MVA, and by about 80% if the VSC loss is further decreased to 0.5% of the nominal VSC capacity. The BCRs have not been calculated in the sensitivity analyses because the estimation of the costs of the VSC having lower losses is not clear yet. It is clear that Case-8 still remains the preferred alternative for the VSC-MTDC system.

4) Loss Reduction Performance of the Selected VSC-MTDC System: To understand how the VSC-MTDC system could contribute to the total system loss reduction, the M-OPF model with the objective function of minimizing the total loss is executed for the case selected in the cost-benefit analysis before (Case-8) under the various load conditions described in Section V-B1 of this paper. The normalized system losses, with respect to the base case, are shown in Fig. 10. It is quite interesting to observe that the total power loss of the mixed ac/dc grid is not always lower than that of the base case. As can be seen in Fig. 10, when the load is lower than about 1.18 times the base case value, the total loss in the mixed ac/dc system is higher than that of the pure ac system. However, as the system is getting more stressed, the total power loss of the mixed ac/dc grid is becoming lower than that of the base case. This is due to the fact that the VSC-MTDC system does help the ac system reduce the power

TABLE V
PARAMETERS OF VSC-MTDC ([24], [34])

VSC station parameters					
S_{nom}	1000 MVA	X_r	0.02 p.u.	A_l	0.12
S_{base}	100 MVA	R_r	0.0001 p.u.	B_l	0.0029
V_{dcnom}	± 300 kV	B_f	2 p.u.	C_l	0.00031
$\overline{I_v}$	10 p.u.	X_{tr}	0.01 p.u.		
		R_{tr}	0.0001 p.u.		

loss under all load conditions. However, the VSC itself introduces power losses which outweigh the reduced loss from the ac system when the system is lightly loaded. The benefit of the VSC-MTDC in reducing power losses is only apparent in heavy loading conditions.

VI. CONCLUSION

In this paper, an extended OPF model incorporating the detailed model of a multiterminal VSC-HVDC (VSC-MTDC) system is proposed. The model is employed as the calculation engine for the proposed cost-benefit analysis to evaluate the benefits offered by the VSC-MTDC embedded into an existing ac transmission system. A case study using a modified Nordic 32-bus system has been performed. The study concludes that the VSC-HVDC systems might lead to reductions in total system operation cost. It is important to note that the reduction of the total system transmission loss depends to a large extent on the VSC-MTDC configuration, and can only be achieved under certain load conditions. The results from sensitivity analyses show that if the VSC loss could be reduced to a third of the original level, the total benefit from the system would be increased by about 70%. A suggestion for the placement and configuration of a VSC-MTDC system is made based on calculated BCRs. To gain a more complete picture of the total benefits rendered by VSC-MTDC projects, additional technical benefits have to be studied and will be the subject of further investigations.

ACKNOWLEDGMENT

The authors would like to thank Dr. A. Edris from Quanta Technology, USA, for his assistance in reviewing the manuscript.

REFERENCES

[1] VSC Transmission CIGRE Working Group B4.37, Tech. Rep., Ref. 269, 2005.
[2] F. Wang, L. Bertling, T. Le, A. Mannikoff, and A. Bergman, "An overview introduction of VSC-HVDC: State-of-art and potential applications in electric power systems," in *Proc. CIGRÈ Int. Symp.*, Bologna, Italy, Sep. 2011.
[3] J. Stefan G, A. Gunnar, J. Erik, and R. Roberto, "Power system stability benefits with VSC DC-transmission systems," in *Proc. CIGRE Conf.*, Paris, France, 2004.
[4] J. Wood and B. F. Wollenberg, *Power Generation Operation and Control*, 2nd ed. New York: Wiley, 1996.
[5] Z. Xiao-Ping, "Multiterminal voltage-sourced converter-based HVDC models for power flow analysis," *IEEE Trans. Power Del.*, vol. 19, no. 4, pp. 1877–1884, Oct. 2004.
[6] J. Beerten, S. Cole, and R. Belmans, "Generalized steady-state VSC MTDC model for sequential AC/DC power flow algorithms," *IEEE Trans. Power Syst.*, vol. 27, no. 2, pp. 821–829, May 2012.
[7] M. Baradar, M. Ghandhari, D. Van Hertem, and A. Kargarian, "Power flow calculation of hybrid AC/DC power systems," presented at the IEEE Power Energy Soc. Gen. Meeting,, San Diego, CA, 2012.
[8] A. Pizano-Martinez, C. R. Fuerte-Esquivel, H. Ambriz-Perez, and E. Acha, "Modeling of VSC-based HVDC systems for a Newton-Raphson OPF algorithm," *IEEE Trans. Power Syst.*, vol. 22, no. 4, pp. 1794–1803, Nov. 2007.
[9] R. Wiget and G. Andersson, "Optimal power flow for combined AC and multi-terminal HVDC grids based on VSC converters," presented at the IEEE Power Energy Soc. Gen. Meeting, San Diego, CA, 2012.
[10] M. Baradar, M. R. Hesamzadeh, and M. Ghandhari, "Modelling of multi-terminal HVDC systems in optimal power flow formulation," presented at the Elect. Power Energy Conf., London, ON, Canada, 2012.
[11] C. Cagigas and M. Madrigal, "Centralized vs. competitive transmission expansion planning: the need for new tools," presented at the IEEE Power Eng. Soc. Gen. Meeting, Toronto, ON, Canada, 2003.
[12] A. L'Abbate, G. Migliavacca, G. Fulli, C. Vergine, and A. Sallati, "The European research project REALISEGRID: Transmission planning issues and methodological approach towards the optimal development of the pan-European system," presented at the Power and Energy Soc. Gen. Meeting, IEEE, San Diego, CA, 2012.
[13] G. Latorre, R. D. Cruz, J. M. Areiza, and A. Villegas, "Classification of publications and models on transmission expansion planning," *IEEE Trans. Power Syst.*, vol. 18, no. 2, pp. 938–946, May 2003.
[14] M. R. Hesamzadeh, N. Hosseinzadeh, and P. J. Wolfs, "Economic assessment of transmission expansion projects in competitive electricity markets—an analytical review," presented at the Univ. Power Eng. Conf., Padova, Italy, 2008.
[15] R. de Dios, F. Soto, and A. J. Conejo, "Planning to expand?," *IEEE Power and Energy Mag.*, vol. 5, no. 5, pp. 64–70, Sep./Oct. 2007.
[16] P. Bresesti, W. L. Kling, R. L. Hendriks, and R. Vailati, "HVDC connection of offshore wind farms to the transmission system," *IEEE Trans. Energy Convers.*, vol. 22, no. 1, pp. 37–43, Mar. 2007.
[17] W. Shu, Z. Jinxiang, T. Lan, and P. Jiuping, "Economic assessment of HVDC project in deregulated energy markets," *Proc. Electric Utility Dereg. Restruct. Power Technol.*, pp. 18–23, 2008.
[18] T. Sousa, M. L. dos Santos, J. A. Jardini, R. P. Casolari, and G. L. C. Nicola, "An evaluation of the HVDC and HVAC transmission economic," presented at the 6th IEEE/PE Transm. Distrib.: Latin America Conf. Expo, Montevideo, Uruguay, 2012.
[19] A. Lotfjou, F. Yong, and M. Shahidehpour, "Hybrid AC/DC transmission expansion planning," *IEEE Trans. Power Del.*, vol. 27, no. 3, pp. 1620–1628, Jul. 2012.
[20] M. Davies, M. Dommaschk, J. Dorn, J. Lang, D. Retzmann, and D. Soerangr, HVDC PLUS—Basics and principle of operation, 2008. [Online]. Available: http://www.energy.siemens.com
[21] C. Du and M. H. J. Bollen, "Power-frequency control for VSC-HVDC during island operation," in *Proc. 8th Inst. Elect. Eng. Int. Conf. AC DC Power Transm.*, 2006, pp. 177–181.
[22] N. Mohan, T. M. Undeland, and W. P. Robbins, *Power Electronics: Converters, Applications, and Design*, 2nd ed. New York: Wiley, 1995.
[23] K. Bhattacharya, M. Bollen, and J. Daalder, *Operation of Restructured Power System*. Norwell, MA: Kluwer, 2001.
[24] G. Daelemans, "VSC HVDC in meshed networks," M.Sc. dissertation, Katholieke University Leuven, Leuven, Belgium, 2008.
[25] *"GAMS—a User's Guide,"* GAMS Development Corp., Washington, DC, USA, Jul. 2011.
[26] *"GAMS—The Solver Manuals,"* GAMS Development Corp., Washington, DC, USA, 2012.
[27] Nord Pool Spot. 2011. [Online]. Available: http://www.nordpoolspot.com/Market-data1/Power-system-data/Consumption1/Consumption/ALL/Hourly1/
[28] *IEA (International Energy Agency), Projected Cost of Generating Electricity*, 2010 ed. Paris, France: IEA.
[29] R. Mohaned, Evaluation of HVDC light as an alternative for the Vancouver Island Transmission Reinforcement (VITR) Project, Appendix Q 2005. [Online]. Available: http://transmission.bchydro.com
[30] K. Walve, *Nordic 32A—a CIGRE Test System for Simulation of Transient Stability and Long Term Dynamics*. Stockholm, Sweden: Svenska Kraftnät, 1994.

[31] C. Grigg, P. Wong, P. Albrecht, R. Allan, M. Bhavaraju, R. Billinton, Q. Chen, C. Fong, S. Haddad, S. Kuruganty, W. Li, R. Mukerji, D. Patton, N. Rau, D. Reppen, A. Schneider, M. Shahidehpour, and C. Singh, "The IEEE reliability test system-1996. a report prepared by the reliability test system task force of the Application of Probability Methods Subcommittee," *IEEE Trans. Power Syst.*, vol. 14, no. 3, pp. 1010–1020, Aug. 1999.

[32] The Energy Market 2004 Swedish Energy Agency, ET 29:2004. Eskilstuna, Sweden, 2004.

[33] in *Personal Communication With a Representative From a VSC-HVDC Manufacturer During the Project Meeting Chalmers University of Technology*, Gothenburg, Sweden, Nov. 7, 2012.

[34] ABB AB, Grid Systems–HVDC, Ludvika, Sweden, It's Time to Connect–a Technical Description of HVDC Light. 2008. [Online]. Available: http://www.abb.com

Wang Feng (S'13) was born in Henan, China, on January 10, 1975. He received the M.Sc. degree in electric power engineering from the Chalmers University of Technology, Gothenburg, Sweden, in 2006, where he is currently pursuing the Ph.D. degree in electric power engineering.

From 2006 to 2010, he was a Senior Engineer with the HVDC Department of ABB (China) Ltd. His research interests include power electronics and its applications in power systems, flexible ac transmission systems, and HVDC.

Anh Le Tuan (S'01–M'09) received the Ph.D. degree in power systems from Chalmers University of Technology, Gothenburg, Sweden, in 2004, and the M.Sc. degree in energy economics from Asian Institute of Technology, Thailand, in 1997.

Currently, he is a Senior Lecturer in the Division of Electric Power Engineering, Department of Energy and Environment, Chalmers University of Technology. His research interests include power system operation and planning, power market and deregulation issues, grid integration of renewable energy, and plug-in electric vehicles.

Lina Bertling Tjernberg (S'98–M'02–SM'08) holds the Chair of Professor in Sustainable Electric Power Systems at Chalmers University of Technology, Gothenburg, Sweden. During 2007–2009, she was with the Swedish Transmission system operator, and from 1997 to 2009, she was associated with KTH, The Royal Technical University in Stockholm. Current research projects are within areas of: smart distribution systems, flexible ac/dc systems, and asset management for wind power systems. She is an Editor for the IEEE TRANSACTIONS ON SMART GRID Technologies

Dr. Bertling is Treasurer of the IEEE Power and Energy Society, and is the Chair of the Swedish PE/PEL Chapter and the IEEE Subcommittee on Risk, Reliability and Probability Applications. She is a member of the Swedish Government Coordination Council for Smart Grid, and an expert for the EU commission within Energy and Security.

Anders Mannikoff (M'10) was born in Alingsås, Sweden, in 1962.

From 1984 to 1994, he was with ASEA/ABB in the field of variable speed drives. At ASEA/ABB, Västeräs, Sweden, he held a number of positions including large drives R&D. In 1994, he joined SP Technical Research Institute of Sweden. At SP, he worked in the fields of product safety, electric power engineering, and metrology. In 2007 he was made Head of the Electrical Measurement Laboratory. The laboratory has the status of national laboratory for electrical quantities, including high voltage and high current.

Anders Bergman (M'10–SM'11) was born in Överluleå, Sweden, in 1948. He received the B.Sc. degree in physics and the Ph.D. degree in high-voltage measurement and test techniques from Uppsala University, Uppsala, Sweden, in 1971.

His thesis focused on "In situ calibration of voltage transformers on the Swedish national grid," which is based on the results of a project to calibrate the total complement of voltage transformers on the Swedish 220- and 400-kV grids. After being involved in the design and construction of a 100-MeV cyclotron at Scanditronix, Uppsala, he moved to the high-voltage laboratory at ASEA, Ludvika, Sweden, in 1977 to be engaged in the metrological aspects of high-voltage testing, with the main emphasis on impulse voltages and partial discharges. Since 1988, he has been with SP Technical Research Institute, Borås, Sweden, where he is responsible for calibration activities of high voltage and high current. He is primarily engaged in calibration activities in fields of high-voltage engineering, which are needed by industry and he has developed several major reference systems that are used for onsite calibration of high-voltage measurement systems. As of 2010, he had coordinated a three-year research project for metrology for HVDC, with participation from eight other European bodies. The project is funded by the European Commission.

Dr. Bergman is involved in international standardization, mainly within IEC TC42, high voltage test techniques, where he is convener of Working Group 20, instruments and software used for measurements in high-voltage and high-current tests. He has received the 1906 award from IEC.